Higher superconducting transition temperature by breaking the universal pressure relation

Liangzi Deng[a,b], Yongping Zheng[c], Zheng Wu[a,b], Shuyuan Huyan[a,b], Hung-Cheng Wu[a,b], Yifan Nie[c], Kyeongjae Cho[c], and Ching-Wu Chu[a,b,d,1]

[a]Texas Center for Superconductivity, University of Houston, Houston, TX 77204; [b]Department of Physics, University of Houston, Houston, TX 77204; [c]Department of Materials Science & Engineering, University of Texas at Dallas, Richardson, TX 75080; and [d]Lawrence Berkeley National Laboratory, Berkeley, CA 94720

By investigating the bulk superconducting state via dc magnetization measurements, we have discovered a common resurgence of the superconducting transition temperatures (T_cs) of the monolayer $Bi_2Sr_2CuO_{6+\delta}$ (Bi2201) and bilayer $Bi_2Sr_2CaCu_2O_{8+\delta}$ (Bi2212) to beyond the maximum T_cs (T_{c-max}s) predicted by the universal relation between T_c and doping (p) or pressure (P) at higher pressures. The T_c of underdoped Bi2201 initially increases from 9.6 K at ambient to a peak at 23 K at 26 GPa and then drops as expected from the universal T_c-P relation. However, at pressures above 40 GPa, T_c rises rapidly without any sign of saturation up to 30 K at 51 GPa. Similarly, the T_c for the slightly overdoped Bi2212 increases after passing a broad valley between 20 and 36 GPa and reaches 90 K without any sign of saturation at 56 GPa. We have, therefore, attributed this T_c resurgence to a possible pressure-induced electronic transition in the cuprate compounds due to a charge transfer between the Cu $3d_{x^2-y^2}$ and the O $2p$ bands projected from a hybrid bonding state, leading to an increase of the density of states at the Fermi level, in agreement with our density functional theory calculations. Similar T_c-P behavior has also been reported in the trilayer $Br_2Sr_2Ca_2Cu_3O_{10+\delta}$ (Bi2223). These observations suggest that higher T_cs than those previously reported for the layered cuprate high-temperature superconductors can be achieved by breaking away from the universal T_c-P relation through the application of higher pressures.

BSCCO | cuprate | high-T_c superconductivity | high pressure | T_c-P relation

Raising the transition temperature (T_c) of superconductors has been a primary driving force behind the sustained effort in superconductivity research ever since its discovery due to the scientific challenges and technological promise that superconductivity at higher temperature can offer. This has been particularly true since the discovery of high-temperature superconductivity (HTS) in the late 1980s (1, 2). The most promising stable HTS systems for higher T_c seem to be the layered cuprates (3), Fe-pnictides (4), and Fe-chalcogenides (4). To date, all known stable HTSs with a T_c above 77 K, the liquid nitrogen boiling point, at ambient or high pressure are perovskite-like layered cuprates. For example, $HgBa_2Ca_2Cu_3O_{8+\delta}$ exhibits the current record T_cs of 134 K (5) at ambient pressure and 164 K above 30 GPa (6, 7). Superconductivity determined resistively has been reported at up to 109 K in unit cell $FeSe/SrTiO_3$ film at ambient pressure (8) (but has not yet been confirmed or reproduced) and at up to 203 K under $\sim$155 GPa (9) and $\sim$260 K under $\sim$190 GPa (10, 11) in H_3S and LaH_{10+x}, respectively, but these compounds are unstable. Superconductivity can be induced in the stable cuprates from their Mott insulating parents by chemical, pressure, photon (12), or electric-field doping (13). It has been found that, independent of the type of doping, the normalized transition temperature (T_c/T_{c-max}) of cuprates varies parabolically with the hole concentration (p) in a universal manner: that is, $(T_c/T_{c-max}) = [1 - 82.6(p - p_o)^2]$ (14), where T_{c-max} is the maximum T_c of a specific compound series when optimally doped with $p = p_o \sim 0.16$ hole per CuO_2 layer. This is in general agreement with the rigid band

model when only small perturbations occur to the electron band structures in their equilibrium state through doping, and doping mainly shifts the Fermi energy as has been demonstrated (e.g., in the $HgBa_2Ca_{n-1}Cu_nO_{2n+2+\delta}$ compound family for $n = 1, 2$, and 3; i.e., for one, two, and three CuO_2 layers per unit cell). The observation of this universal T_c/T_{c-max}-p (or -P) behavior suggests that the usual doping (chemical p or pressure P) of cuprates in their equilibrium state cannot lead to a T_c higher than T_{c-max}. To achieve a T_c higher than T_{c-max} in cuprates, one may have to modify their electronic structures, such as by inducing a Fermi surface topology change (15, 16) via very high pressures (i.e., $P >> \sim$20 GPa, the pressure that most previous experiments on cuprates have reached). In other words, we have to break away from the commonly accepted universal T_c-p (or T_c/T_{c-max}-p or T_c/T_{c-max}-P) relation.

To explore such a possibility, we have investigated the high-pressure effects on the T_cs of members of the homologous series of $Bi_2Sr_2Ca_{n-1}Cu_nO_{2n+4+\delta}$ (BSCCO) (Fig. 1D) with $n = 1$ and 2, where n is the number of CuO_2 layers per cell, magnetically up to $\sim$56 GPa. Indeed, we have observed the resurgence of their T_cs at higher pressures after reaching the T_{c-max} predicted by the universal quadratic (T_c/T_{c-max}-p) relation. Similar T_c resurgence under high pressure has also been reported in the optimally doped $Br_2Sr_2Ca_2Cu_3O_{10+\delta}$ (Bi2223) with $n = 3$ by Chen et al. (17), although the authors attributed the T_c rise to the possible pressure-induced competition between the pairing and phase

---

Significance

Achieving higher transition temperature (T_c) is a primary goal in superconductivity research. T_c and doping have been found to have a dome-like universal relation where the peak position is the maximum T_{c-max}, which is consistent with previous experimental results in the lower pressure range. By using the ultrasensitive magnetization measurement technique under high pressure that we developed, we discovered a universal resurgence of T_c passing the peak predicted by the general T_c-p (doping) or -P (pressure) relation for cuprate high-temperature superconductor and attribute the resurgence to a pressure-induced electronic transition, which is supported qualitatively by our density functional theory calculations. This offers a paradigm to raise the T_c of the layered cuprate high-temperature superconductors to a new height.

www.manaraa.com

ordering among the three different CuO_2 planes specific to Bi2223. Our experiments show that the resurgence of T_c beyond the T_{c-max} clearly is n independent and seems to be common to layered cuprates, probably due to a pressure-induced electronic transition that gives rise to the increase of the electron density of states (DOS) at the Fermi level, consistent with our density functional theory (DFT) calculations.

Pressure has played a crucial role in the development of HTS due to its simplicity in varying the basic parameter of solids, the interatomic distance, without introducing complications associated with altering the chemistry of the compound. The close relationship between pressure and doping has been demonstrated experimentally and explained theoretically (18, 19). The universal T_c-p relation can, therefore, be replaced by the
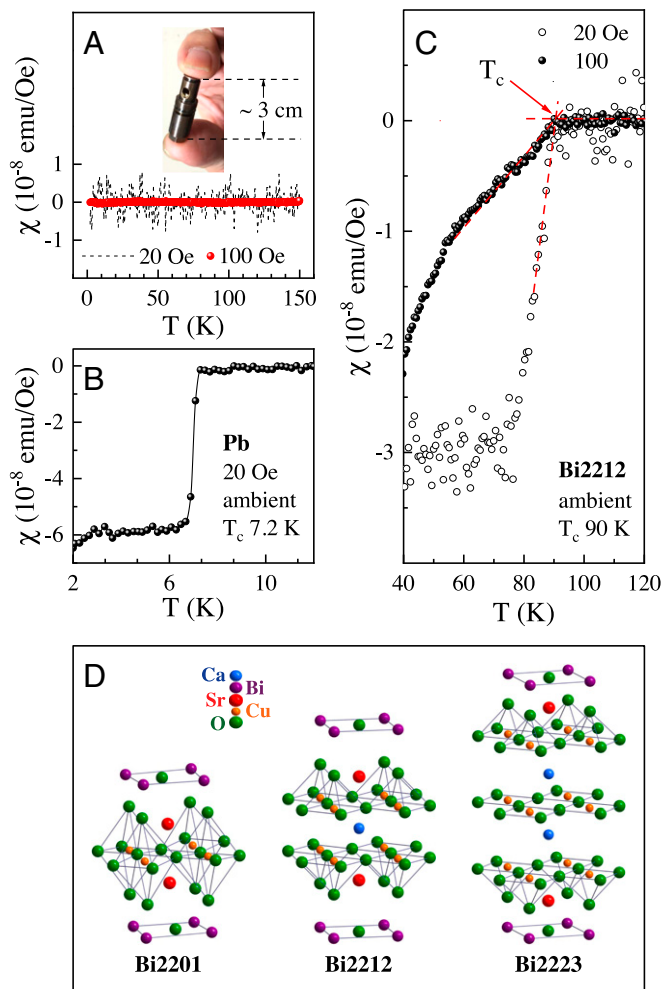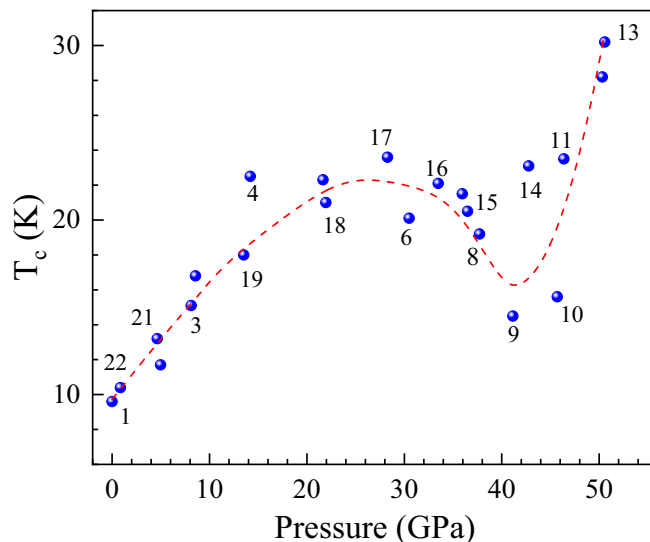

Fig. 2. Pressure dependence of T_c in underdoped Bi2201. The T_cs were determined by dc magnetization measurements. The numbers represent the sequential order of the experimental runs during both loading and unloading processes. The T_{c-max} is found to be ~23 K at a pressure of ~26 GPa. T_c at pressures above 40 GPa rises rapidly without any sign of saturation up to 30 K at 51 GPa, which is the highest pressure applied. The red dashed line is a guide for the eyes.

universal T_c-P relation. For instance, it was the anomalously large positive pressure effect on the T_c of the first cuprate superconductor, $(La,Ba)_2CuO_4$ (20, 21), that prompted the substitution of the smaller ion Y^{3+} for La^{3+} to generate lattice pressure, leading to the discovery of the first liquid nitrogen HTS: $YBa_2Cu_3O_{7+\delta}$ (2). It was also the high pressure of ~31 GPa that helped achieve the current record high T_c in $HgBa_2Ca_2Cu_3O_{8+\delta}$ (6, 7). Pressure on a compound can change its carrier concentration and shift its Fermi level, and it can sometimes even alter its Fermi surface topology, leading to a Lifshitz transition (15, 16). It has been demonstrated that $d\ln T_c/dP$ is positive for underdoped HTSs, negative for overdoped HTSs, and approximately zero for optimally doped HTSs (22) in agreement with the universal $T_c(p)$, at least at low pressure (e.g., <20 GPa). This is because, within the framework of the rigid band model, dT_c/dP can be written as $dT_c/dP = (dT_c/dp)(dp/dP)$. By assuming a positive dp/dP, the sign change of dT_c/dP with p is determined by the sign of the slope of $T_c(p)$ and can thus be understood.

Results

Recently, we developed an ultrasensitive high-pressure miniature diamond anvil cell (mini-DAC) technique (Fig. 1A) that enables us to investigate the bulk superconducting state of a solid with ≤100-μm diagonal by directly measuring the dc magnetization under pressures up to ~60 GPa. We used this technique to investigate the bulk superconducting states of the underdoped $Bi_2Sr_2CuO_{6+\delta}$ (Bi2201) and the nearly optimally doped $Bi_2Sr_2CaCu_2O_{8+\delta}$ (Bi2212). The pressure dependences of T_c are shown in Figs. 2 and 3. The T_cs were determined by dc magnetization measurements (*SI Appendix*, Figs. S1 and S2). As shown in Fig. 2, the T_c of the underdoped Bi2201 initially increases rapidly from 9.6 K at ambient to a peak at ~23 K (T_{c-max}) at ~26 GPa and then drops to ~15 K at ~40 GPa as expected for an underdoped cuprate HTS in accordance with the universal T_c-P relation. However, T_c at pressures above 40 GPa rises rapidly without any sign of saturation up to 30 K at 51 GPa, the highest pressure applied, at a rate of ~+1.5 K/GPa in contrast to the continued drop with pressure

Fig. 1. The dc susceptibility measurements with a mini-DAC at ambient pressure. (*A*) The homemade mini-DAC with diameter of ~8.8 mm and length of ~3 cm was developed to be adapted to the Quantum Design MPMS 3 for ultrasensitive magnetization measurements. Background measurements were taken under 20 Oe and 100 Oe before loading samples into the mini-DAC. The variance of different runs of background measurements is below 2×10^{-8} emu/Oe. (*B*) Measurement of a calibration Pb sample with diagonal ~100 μm and thickness below 10 μm at 20 Oe. A sharp superconducting transition at 7.2 K was detected. (*C*) Measurement of a Bi2212 single crystal with diagonal ~80 μm and thickness below 10 μm. A superconducting transition at 90 K was observed for measurements under both 20 and 100 Oe, while the 100-Oe measurement shows a better signal-to-noise ratio. We have, therefore, chosen the onset T_c at 100 Oe as the T_c in this study. The red dashed lines are used for $T_{c-onset}$ extrapolation. (*D*) Schematic of the crystal structure of $Bi_2Sr_2Ca_{n-1}Cu_nO_{2n+4+\delta}$ with $n = 1$, 2, and 3.
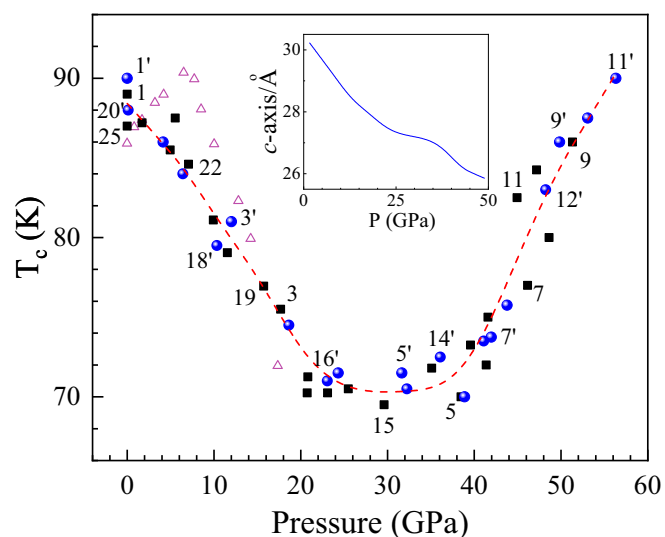
Deng et al.

www.manaraa.com

Fig. 3. Pressure dependence of T_c in slightly overdoped Bi2212. T_cs were determined by dc magnetization measurements. The two sets of numbers (without and with primes) represent the sequential orders of the experimental runs for two single-crystal samples, with squares representing sample 1 and circles representing sample 2. The triangles are from ref. 23 for slightly underdoped Bi2212. After passing a U-shaped valley under pressure of 20–36 GPa, T_c rises rapidly without any sign of saturation to ~90 K at ~56 GPa, which is the highest pressure applied. The red dashed line is a guide for the eyes. *Inset* shows the *c*-lattice parameter of Bi2212 under pressures up to 50 GPa from ref. 24.

predicted by the universal T_c-P relation. It is evident that the pressure effect observed is rather reversible. Fig. 3 shows the T_c behavior under pressures reversibly for two single-crystalline samples of Bi2212. The sample is slightly overdoped as evidenced by its slightly lower T_c. The T_c-P behavior is qualitatively similar to that of Bi2201 at high pressures after reaching its $T_{c\text{-max}}$. Under pressure, T_c decreases rapidly from ~90 K at ambient to ~71 K at ~20 GPa as expected for an overdoped cuprate HTS based on the universal T_c-P relation. It continues to decrease but at a slower rate above ~20 GPa, passes a broad minimum of ~69 K at ~30 GPa, and finally, rises rapidly after ~40 GPa to ~90 K at ~56 GPa, the highest pressure applied, at a rate of ~+1.4 K/GPa. As shown in Fig. 3, the low-pressure effect on the T_c of our samples does not result in the peak previously reported by Chen et al. (23). We attribute the difference to the different doping levels of the samples studied [i.e., our samples are slightly overdoped, while the sample of Chen et al. (23) is slightly underdoped, which may require a higher pressure to induce a resurgence of T_c]. Our observations show that, while the T_c of Bi2201 and Bi2212 under low pressures (e.g., <20 GPa) behaves in accordance with the universal T_c-P relation, a higher T_c emerges at higher pressures, possibly associated with a subtle change of the electron energy structures characteristic of the CuO$_2$ layers in cuprates. In fact, similar T_c-P behavior has also been reported in Bi2223 (17) with the triple-CuO$_2$ layers per unit cell [i.e., under pressure, its T_c increases from

108 K at ambient, peaks at 123 K ($T_{c\text{-max}}$) at 12 GPa, decreases to 118 K at 23 GPa, and finally, increases to 136 K at 36 GPa at a rate of ~+1.4 K/GPa]. The final T_c increase at high pressures was ascribed by Chen et al. (17) to a pressure-driven transition of the inner CuO$_2$ layer from the competing order to a superconducting state, thus specific to the triple-CuO$_2$ layer cuprates. However, we attribute the T_c rise at higher pressure after reaching its peak to an electronic transition generic to the CuO$_2$ layers in cuprates under very high pressures, independent of the number of CuO$_2$ layers per unit cell as summarized in Table 1. It is interesting to note that, after the T_c resurgence for Bi2201, Bi2212, and Bi2223, their dT_c/dP values are large and rather similar, but the sign of the dT_c/dP at low pressures depends on the compound's initial doping state. The observations, therefore, suggest that higher T_cs than those previously reported in layered cuprate HTSs can be achieved by breaking away from the universal T_c-P relation via inducing a transition in the electronic spectrum of the CuO$_2$ layer by the application of higher pressures.

Numerous structural studies on BSCCO have been made under pressures up to 50 GPa at room temperature (17, 24–26). None have displayed any pressure-induced structure transition, although charge redistribution within the cell under pressure has been suggested from the Raman studies (17). The absence of any pressure-induced structure transition is consistent with our proposed electronic transition, such as the Lifshitz transition (15, 16), which may not be accompanied by a structural change. However, despite the absence of a structural transition, anomalies appear in the *c*-lattice parameter of Bi2212 at ~30 GPa (24), coinciding with the broad U-shaped T_c valley that we have observed as shown in Fig. 3, *Inset*.

Discussion

In searching for the microscopic origin of the unusual pressure enhancement effect on T_c, we have performed quantum mechanical computations based on the DFT + U method, where the Hubbard U term is used to treat the strong onsite Coulomb interaction of localized Cu 3d electrons on Bi2201 and Bi2212. The excess oxygen δs are estimated, according to the T_c-δ relation, to be 0.17 (27) and 0.25 (28) for Bi2201 (T_c ~ 10 K) and Bi2212 (T_c ~ 90 K), respectively. Our calculations show that the excess oxygen δ resides energetically favorably between the BiO layers. Both hydrostatic and nonhydrostatic pressures were applied to shrink the supercell volume while allowing the shape of the supercell to relax. The experimental compressibility values of the a and c axes were used as the input for the nonhydrostatic case (24, 25). We have calculated the total DOS, the partial DOS, and the band structures near the Fermi level at selected pressures. Fermi surface topology changes are induced by pressures above ~37 GPa for Bi2201 and above ~42 GPa for Bi2212 as shown in *SI Appendix*, Fig. S3. The projected electronic band Cu 3$d_{x^2-y^2}$ variations with pressure are displayed in Fig. 4 *A* and *B*. The accompanying evolutions of the band-state occupancy with pressures are shown in Fig. 4*C*. The DOSs vary with pressure in a fashion qualitatively similar to that with the T_cs. For these compounds, the calculations also clearly show that pressure inhomogeneity has a rather large effect on the electronic transition as

Table 1. dT_c/dP for BSCCO with n = 1, 2, and 3 under different pressure ranges

Bi2201	Bi2212	Bi2223
0–26 GPa: +0.5 K/GPa	0–22 GPa: −0.9 K/GPa	0–12 GPa: +1.3 K/GPa
26–41 GPa: −0.4 K/GPa	22–42 GPa: ±0.2 K/GPa	12–23 GPa: −0.5 K/GPa
41–51 GPa: +1.5 K/GPa	**42–56 GPa: +1.4 K/GPa**	**23–36 GPa: +1.4 K/GPa**

The dT_c/dP values for Bi2223 were estimated from the results reported in ref. 17. For Bi2201, Bi2212, and Bi2223, the signs and magnitudes of dT_c/dP at low pressures depend on the compound's initial doping state, and the dT_c/dP values at higher pressures, after the T_c resurgences, are large and rather similar. Boldface text is used to emphasize the dT_c/dP at the pressure range where the T_c-resurgence took place.
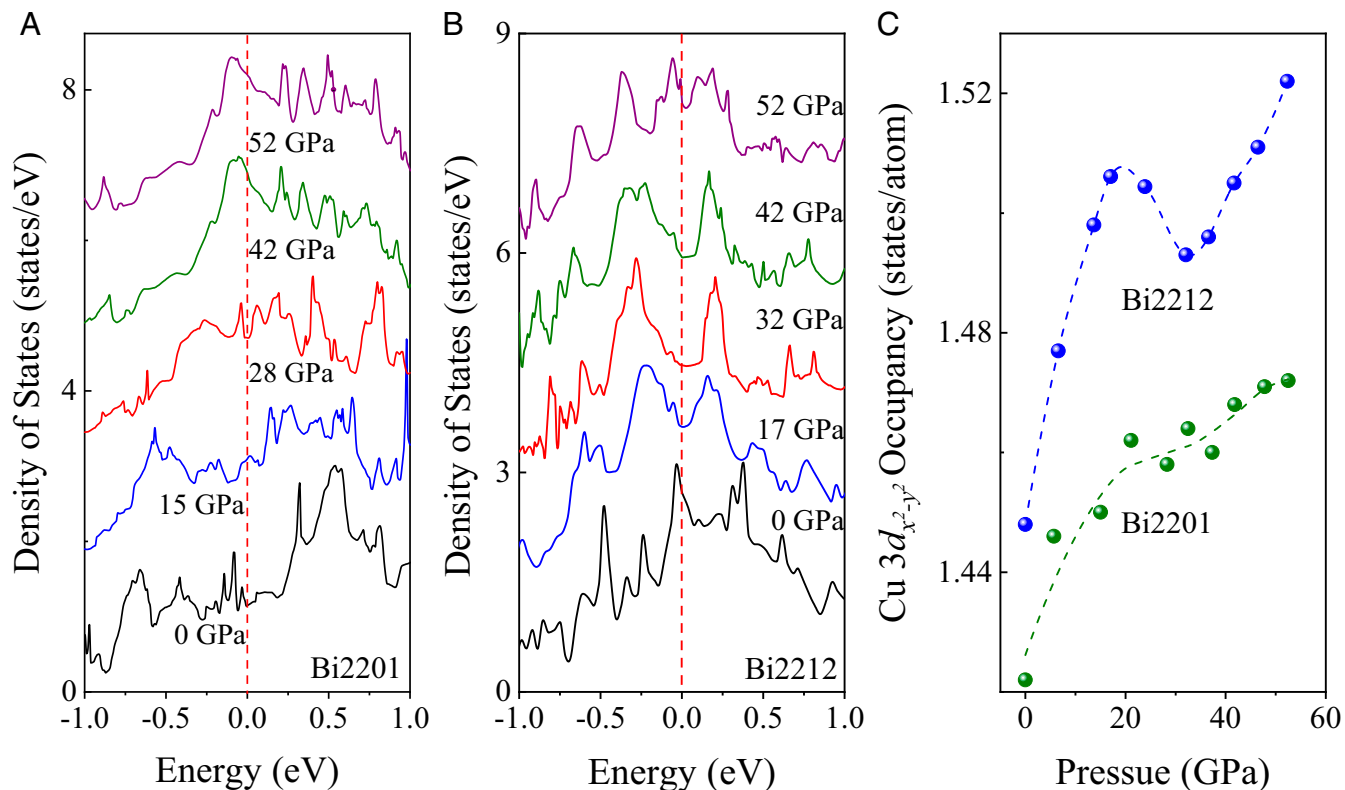
Fig. 4. Evolution of the projected Cu $3d_{x^2-y^2}$ bands under pressure. Band shifting with respect to the Fermi level under pressures from ambient up to 52 GPa: (*A*) Bi$_2$Sr$_2$CuO$_{6.17}$ (Bi2201) and (*B*) Bi$_2$Sr$_2$CaCu$_2$O$_{8.25}$ (Bi2212). Curves are shifted up vertically. (*C*) Pressure dependence of band states occupancy defined as the total states below the Fermi level of the projected Cu $3d_{x^2-y^2}$ band in Bi2201 and Bi2212. A charge transfer process exists during the compression of the Cu–O bond, which causes the Fermi level to right shift to allow more occupied states. The DOSs vary with pressure in a fashion qualitatively similar to that of the T_cs. The Fermi level is set to zero.

displayed in Fig. 5 (i.e., the pressure inhomogeneity tends to induce the transition at lower pressure). The calculated DOSs under nonhydrostatic pressures more closely reproduce the T_c-P behavior observed. This effect has been reported experimentally in HTSs previously (29, 30). Our experimental results and theoretical calculations as summarized in *SI Appendix*, Table S1 suggest that it is possible to reach T_cs even higher than what we obtained in experiments by continuing to push the applied pressure limit.

Detailed structural studies and transport properties associated with the observed superconducting behaviors are currently being

conducted. It would also be interesting to investigate the scaling between T_c and the superfluid density (31) under high pressure in the BSCCO system.

In conclusion, we have observed that the T_cs of layered cuprates Bi2201 and Bi2212 increase beyond the maximum T_c predicted by the universal T_c-P relation under high pressures, independent of the number of CuO$_2$ layers per formula. We have attributed the T_c resurgence to a pressure-induced electronic transition in the CuO$_2$ layers of the cuprate HTSs (e.g., a Fermi surface topology change) in qualitative agreement with our DFT + U
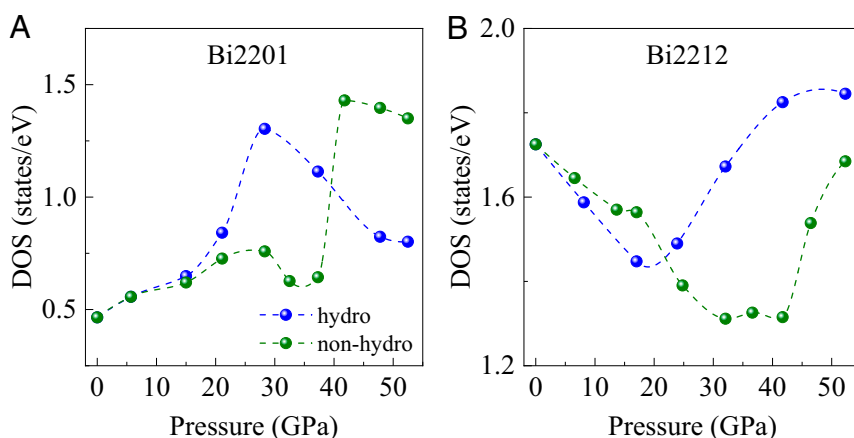

Fig. 5. Evolution of DOS at the Fermi level under pressure. Total electronic DOS under hydrostatic (blue) and nonhydrostatic (green) conditions: (*A*) Bi$_2$Sr$_2$CuO$_{6.17}$ (Bi2201) and (*B*) Bi$_2$Sr$_2$CaCu$_2$O$_{8.25}$ (Bi2212). The calculated DOSs under nonhydrostatic pressures more closely reproduce the T_c-P behavior observed.

Deng et al.

www.manaraa.com

calculations. The observations, therefore, provide a path to higher T_cs than previously achieved in layered cuprates by breaking away from the universal T_c-P relation. They will certainly stimulate future experimental and theoretical investigations on the T_c resurgence in other cuprates as well as in Fe-based superconductors.

Materials and Methods

Crystal Growth. The polycrystalline Bi2201 was prepared by the standard solid-state method followed by a prolonged oxygen annealing. The stoichiometric mixture of high-purity Bi_2O_3 (99.9995%), $SrCO_3$ (99.99%), and CuO (99.995%) was pressed into a pellet and then sintered in a temperature range from 700 °C to 850 °C in oxygen atmosphere. This procedure was repeated at least four times with intermediate grinding. It displayed a superconducting transition around 10 K similar to that previously reported (27). The single-crystalline Bi2212 was grown by the floating zone technique (32).

dc Magnetization Measurements Under High Pressure. We developed a mini-DAC fabricated from BeCu alloy with length of ~3 cm and outer diameter of ~8.8 mm, which was adapted into a Quantum Design Magnetic Property Measurement System (MPMS) for ultrasensitive magnetization measurements at temperatures down to 1.8 K and in fields up to 7 T under high pressure. A pair of 300-μm-diameter culet-sized diamond anvils was used for all of the measurements under high pressure. The gaskets are made from nonmagnetic Ni–Cr–Al alloy. Each gasket was preindented to ~20–40 μm in thickness, and a 100- to 120-μm-diameter hole was drilled to serve as the sample chamber. Thermal grease was used as the pressure-transmitting medium. The applied pressure was measured by the fluorescence line of ruby powders and the Raman spectrum from the culet of the top diamond anvil. Samples with diagonal ~80–100 μm and thickness of a few micrometers were prepared to provide a sufficient magnetic signal. The reproducibility of the background signal under different magnetic fields and thermal cycles was confirmed. The variance of different runs of background measurements is below 2×10^{-8} emu/Oe, which offers a good platform to analyze the superconducting signal under high pressure. A piece of calibration Pb sample with diagonal ~100 μm was tested with the mini-DAC at ambient pressure. A sharp superconducting transition at 7.2 K was detected.

Density Functional Calculations. The Vienna ab initio simulation package (33, 34) with the projector-augmented wave method (35) was used for all of the calculations in this study. The plane wave cutoff energy was set to 450 eV, and the generalized gradient approximation (GGA) with the semilocal Perdew–Burke–Ernzerhof (36) function was adopted to describe the exchange correlation interactions. The Brillouin zone was sampled with Γ-centered k meshes with a spacing of 0.027 $Å^{-1}$ for the crystal structure optimization and 0.013 $Å^{-1}$ for the electronic structure calculations. The tetrahedron method with Blöchl corrections was carried out to obtain the accurate DOS. The criteria of convergence for energy and force were set to 10^{-5} eV and 0.005 eV/Å, respectively. Onsite Coulomb repulsion of Cu 3d electrons was corrected by the GGA + U method (37), with U_{eff} = 4 eV according to previous theoretical reports (38).

In the hydrostatic model, lattice parameters under different pressures are obtained by shrinking the supercell under free relaxation of the lattice parameters with fixed volumes. Under these conditions, the pressures along each direction are the same (i.e., homogeneous pressure). However, the difference between our theoretical lattice parameters under hydrostatic conditions and the reported lattice parameters measured by synchrotron X-ray diffraction (24, 25) indicates that the actual pressure along the ab plane is smaller than that along the c axis above a certain pressure, which is affected by the hydrostatic limit of the pressure-transmitting medium as well as the strength anisotropy of the testing material. To better simulate the inhomogeneous pressure condition, we used the experimental data as a reference to adjust the pressure along different directions accordingly.

1. Bednorz JG, Müller KA (1986) Possible high T_c superconductivity in the Ba–La–Cu–O system. *Z Phys B* 64:189–193.
2. Wu MK, et al. (1987) Superconductivity at 93 K in a new mixed-phase Yb-Ba-Cu-O compound system at ambient pressure. *Phys Rev Lett* 58:908–910.
3. Chu CW, Deng LZ, Lv B (2015) Hole-doped cuprate high temperature superconductors. *Physica C* 514:290–313.
4. Hosono H, Yamamoto A, Hiramatsu H, Ma YW (2018) Recent advances in iron-based superconductors toward applications. *Mater Today* 21:278–302.
5. Schilling A, Cantoni M, Guo JD, Ott HR (1993) Superconductivity above 130 K in the Hg–Ba–Ca–Cu–O system. *Nature* 363:56–58.
6. Chu CW, et al. (1993) Superconductivity above 150 K in $HgBa_2Ca_2Cu_3O_{8+\delta}$ at high pressures. *Nature* 365:323–325.
7. Gao L, et al. (1994) Superconductivity up to 164 K in $HgBa_2Ca_{m-1}Cu_mO_{2m+2+\delta}$ (m=1, 2, and 3) under quasihydrostatic pressures. *Phys Rev B Condens Matter* 50:4260–4263.
8. Ge JF, et al. (2015) Superconductivity above 100 K in single-layer FeSe films on doped $SrTiO_3$. *Nat Mater* 14:285–289.
9. Drozdov AP, Eremets MI, Troyan IA, Ksenofontov V, Shylin SI (2015) Conventional superconductivity at 203 kelvin at high pressures in the sulfur hydride system. *Nature* 525:73–76.
10. Drozdov AP, et al. (2018) Superconductivity at 215 K in lanthanum hydride at high pressures. arXiv:1808.07039v1.
11. Somayazulu M, et al. (2018) Evidence for superconductivity above 260 K in lanthanum superhydride at megabar pressures. arXiv:1808.07695v1.
12. Demsar J (2016) Light-induced superconductivity. *Nat Phys* 12:202–203.
13. Lei B, et al. (2016) Evolution of high-temperature superconductivity from a low-T_c phase tuned by carrier concentration in FeSe thin flakes. *Phys Rev Lett* 116:077002.
14. Presland MR, Tallon JL, Buckley RG, Liu RS, Flower NE (1991) General trends in oxygen stoichiometry effects on T_c in Bi and Tl superconductors. *Physica C* 176:95–105.
15. Lifshitz IM (1960) Anomalies of electron characteristics of a metal in the high pressure region. *Sov Phys JETP* 11:1130–1135.
16. Chu CW, Smith TF, Gardner WE (1968) Superconductivity of rhenium and some rhenium-osmium alloys at high pressure. *Phys Rev Lett* 20:198–201.
17. Chen XJ, et al. (2010) Enhancement of superconductivity by pressure-driven competition in electronic order. *Nature* 466:950–953.
18. Ambrosch-Draxl C, Sherman EY, Auer H, Thonhauser T (2004) Pressure-induced hole doping of the Hg-based cuprate superconductors. *Phys Rev Lett* 92:187004.
19. Sakakibara H, et al. (2013) First-principles band structure and FLEX approach to the pressure effect on T_c of the cuprate superconductors. *J Phys Conf Ser* 454:012021–012028.
20. Chu CW, et al. (1987) Evidence for superconductivity above 40 K in the La-Ba-Cu-O compound system. *Phys Rev Lett* 58:405–407.
21. Chu CW, Hor PH, Meng RL, Gao L, Huang ZJ (1987) Superconductivity at 52.5 k in the lanthanum-barium-copper-oxide system. *Science* 235:567–569.
22. Chu CW, et al. (1991) High pressure study of high temperature superconductors: Material base, universal T_c-behavior, and charge transfer. *Frontiers of High-Pressure Research*, eds Hochheimer HD, Etters RD (Plenum, New York), p 383.
23. Chen XJ, Struzhkin VV, Hemley RJ, Mao HK, Kendziora C (2004) High-pressure phase diagram of $Bi_2Sr_2CaCu_2O_{8+\delta}$ single crystals. *Phys Rev B Condens Matter Mater Phys* 70:214502.
24. Olsen JS, Steenstrup S, Gerward L, Sundqvist B (1991) High pressure studies up to 50 GPa of Bi-based high-T_c superconductors. *Phys Scr* 44:211–213.
25. Zhang JB, et al. (2013) Pressure-induced isostructural phase transition in $Bi_2Sr_2CaCu_2O_{8+\delta}$. *Chin Phys C* 37:088003.
26. Akhtar ZN, Akhtar MJ, Clark SM, Catlow CRA (1994) The effect of pressure on the crystal structures of some bismuth based superconductors. *Solid State Commun* 92:535–540.
27. Kato M, Yoshimura K, Kosuge K (1997) Evidence for antiferromagnetic order in $Bi_2Sr_2CuO_6$. *J Solid State Chem* 133:372–378.
28. Deshimaru Y, Otani T, Shimizu Y, Miura N, Yamazoe N (1991) Influence of oxygen content on the superconductivity of Bi-based oxides homologous to 2212 phase. *Jpn J Appl Phys* 30:L1798–L1801.
29. Torikachvili MS, Bud'ko SL, Ni N, Canfield PC (2008) Pressure induced superconductivity in $CaFe_2As_2$. *Phys Rev Lett* 101:057006.
30. Yu W, et al. (2009) Absence of superconductivity in single-phase $CaFe_2As_2$ under hydrostatic pressure. *Phys Rev B Condens Matter Mater Phys* 79:020511.
31. Božović I, He X, Wu J, Bollinger AT (2016) Dependence of the critical temperature in overdoped copper oxides on superfluid density. *Nature* 536:309–311.
32. Takekawa S, Nozaki H, Umezono A, Kosuda K, Kobayashi M (1988) Single crystal growth of the superconductor $Bi_{2.0}(Bi_{0.2}Sr_{1.8}Ca_{1.0})Cu_2O_8$. *J Cryst Growth* 92:687–690.
33. Kresse G, Hafner J (1993) Ab initio molecular dynamics for liquid metals. *Phys Rev B Condens Matter* 47:558–561.
34. Kresse G, Furthmuller J (1996) Efficiency of ab-initio total energy calculations for metals and semiconductors using a plane-wave basis set. *Comput Mater Sci* 6:15–50.
35. Kresse G, Joubert D (1999) From ultrasoft pseudopotentials to the projector augmented-wave method. *Phys Rev B Condens Matter Mater Phys* 59:1758–1775.
36. Perdew JP, Burke K, Ernzerhof M (1996) Generalized gradient approximation made simple. *Phys Rev Lett* 77:3865–3868.
37. Dudarev SL, Botton GA, Savrasov SY, Humphreys CJ, Sutton AP (1998) Electron-energy-loss spectra and the structural stability of nickel oxide: An LSDA+U study. *Phys Rev B Condens Matter Mater Phys* 57:1505–1509.
38. Wang L, Maxisch T, Ceder G (2006) Oxidation energies of transition metal oxides within the GGA+U framework. *Phys Rev B Condens Matter Mater Phys* 73:195107.

www.manaraa.com